Synthesis of Nickel-doped Transparent Glass-ceramics for Ultra-broadband Optical Fiber Amplifiers

Takenobu Suzuki, Yusuke Arai, and Yasutake Ohishi

Research Center for Advanced Photon Technology, Toyota Technological Institute, 2-12-1, Hisakata, Tempaku-ku, 468-8511 Nagoya, Japan.

E-mail: takenobu@toyota-ti.ac.jp, ohishi@toyota-ti.ac.jp

Abstract: The structural and optical properties of Ni-doped transparent glass-ceramics are reviewed. The quantum efficiencies of ceramics were examined to explore suitable crystalline phase for Ni-doping in glass-ceramics. Inverse spinel $LiGa_5O_8$ have the quantum efficiency of almost 100 % at room temperature. Transparent glass ceramics containing $LiGa_5O_8$ was successfully synthesized by heat treatment of Li_2O-Ga_2O_3-SiO_2-NiO glass. Most of Ni^{2+} ions in glass-ceramic were incorporated into $LiGa_5O_8$ nanocrystals. The near-infrared emission covering from the O-band to L-band (1260 – 1625 nm) was observed from the Ni-doped Li_2O-Ga_2O_3-SiO_2 glass-ceramic though it was not observed from the as-cast glass. The lifetime of the emission was about 580 μsec even at 300K. The emission quantum efficiency was evaluated as about 10 % that is enough high for practical usage as gain media of optical fiber amplifiers. The figure of merit (the product of the stimulated emission cross section and lifetime) was as high as that of rare-earth-doped glasses. The broad bandwidth, high quantum efficiency and high figure of merit show that transparent glass-ceramics containing Ni^{2+}:$LiGa_5O_8$ nanocrystals are promising candidates as novel ultra-broadband gain media.

1. Introduction

Broadband optical amplifiers are key devices for the development of dense wavelength-division-multiplexing (DWDM) network systems. Many efforts have been made to realize ultra-broadband optical amplification for DWDM use using rare-earth-doped fibers, fiber Raman amplifiers and their hybridized systems. Transition metal ions have a potential as active ions for ultra-broadband optical amplification. Non-radiative decay processes dominate the relaxations of the excited states of transition metals and the quantum efficiency of transition metals is very low in glasses, though they can have sufficiently large quantum efficiency in single crystals[1]. However, it is difficult to make single crystals fiber form. In contrast, glasses can be easily obtained as large size bulk and used as fiber and waveguide materials. Glass-ceramics are of interest as hosts for transition metals, since they have the advantage of both mechanical properties like glass materials and optical activities like single crystalline materials. If the sizes of crystallites in glass-ceramics are far less than the wavelength of interest, the light scattering caused by the crystals would be negligible. Such glass-ceramics are known as transparent glass-ceramics. Furthermore, if transition metal ions are included in crystallites glass-ceramics, it is expected that the quantum efficiency of the broadband emissions becomes high like in single crystals.

Broadband emission located around 1300 nm with over 200 nm bandwidth from Ni^{2+}-doped nanocrystals embedding transparent glass-ceramics has been reported[2-6]. These glass-ceramics are expected to be potential candidates as gain media for ultra-broadband optical fiber amplifiers, tunable lasers and ultra short pulse lasers in telecommunication wavelength regions.

In this paper, we will review the structural and optical properties of Ni-doped transparent glass-ceramics.

2. Selection of Ni^{2+}-doped Crystals Embedded in Glass-ceramics

At fast, we investigate near-infrared emissions of various Ni^{2+}-doped oxide crystals so as to explore suitable crystalline phase to be grown in the glass-ceramics. The peak wavelength, full width at the half maximum lifetime and quantum efficiency of NIR emissions from Ni-doped oxide crystals are summarized in Table 1 These materials can be classified into four groups as (1) aluminate and gallate spinels ($ZnGa_2O_4$, $ZnAl_2O_4$, $MgGa_2O_4$, $MgAl_2O_4$ and $LiGa_5O_8$), (2) periclase (MgO), (3) titanate spinels (Mg_2TiO_4 and Zn_2TiO_4) and (4) olivines (Mg_2SiO_4, Mg_2GeO_4). Even though Ni:MgO is lasable, this material is not useable for our objective because it can not be precipitated in glass. Titanate spinels and olivines give rise to a NIR emission located at relatively longer wavelength and the lifetime is far shorter than that of the other materials. De-excitation process of titanate spinels and olivnes should be dominated by non-radiative transition through the intermediary of phonons. The quantum efficiency of the NIR emission of titanate spinels and olivines is very low. Aluminate and gallate spinels show a NIR emission located at relatively shorter wavelength with longer lifetime. These materials have relatively high quantum efficiency probably due to higher ionicity (or lower covalency) of chemical bonds in alluminate and gallate spinels than titanate spinels and olivines. It is thought that $LiGa_5O_8$ is the most suitable among alluminate and gallate spinels because of the extremely high quantum efficiency (~100 %) at room temperature. Furthermore, It has been reported that $LiGa_5O_8$ nanocrytals could be precipitated from silicate glass[7-9]. We selected, therefore, $LiGa_5O_8$ is the most suitable candidate crystalline phase for transparent glass-ceramics embedding Ni^{2+}-doped nanocrystals.

Table I. The peak wavelength, full width at the half maximum (FWHM), lifetime and quantum efficiency of NIR emissions from Ni-doped oxide crystals at room temperature

Host material	Peak wavelength [nm]	FWHM [nm]	Lifetime at 300 K [msec]	Quantum efficiency .h[%]
aluminate and gllate spinels				
$ZnGa_2O_4$	1230	300	60	~18
$ZnAl_2O_4$	1240	220	100	~19
$MgGa_2O_4$	1260	280	1200	95
$MgAl_2O_4$	1280	200	300	~20
$LiGa_5O_8$	1300	250	1700	~100
periclase				
MgO	1330	230	4000	~80
titanate spinels				
Mg_2TiO_4	1400	320	<10	-
Zn_2TiO_4	1420	310	<10	-
olivines				
Mg_2SiO_4	1500	250	40	~1
Mg_2GeO_4	1550	250	<10	<1

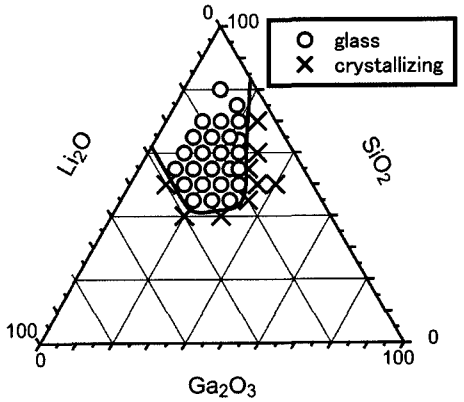

Fig. 1. Glass forming region of 30 g batch of Li_2O-Ga_2O_3-SiO_2-0.1NiO quasi-ternary system at a cooling rate of roughly about 10 K/sec[7].

3. Preparation of Nickel-doped Transparent Glass-ceramics

3.1. Glass Forming Region

Fig. 1 shows a phase diagram depicting various compositions in the Li_2O-Ga_2O_3-SiO_2-0.1NiO quasi-ternary system. In the present study, the NiO content was kept at a constant concentration of 0.1 mol%. Transparent glass samples are yielded for compositions indicated by open circles in Fig. 1. The glass forming region was bounded by $SiO_2 \geq 40$, $Li_2O \leq 40$ and $(Ga_2O_3 - Li_2O) \leq 15$ in mol%. Transparent glass-ceramic was obtained from the sample of the composition of $13Li_2O$-$23Ga_2O_3$-$64SiO_2$-0.1NiO (in mol%) after an appropriate post heat treatment. So we concentrated our attention on the properties of this composition.

3.2. Heat Treatment Condition to Prepare Transparent Glass-ceramics

Fig. 2 shows the change of XRD patterns with the heat treatment temperature. The heat treatment was car-

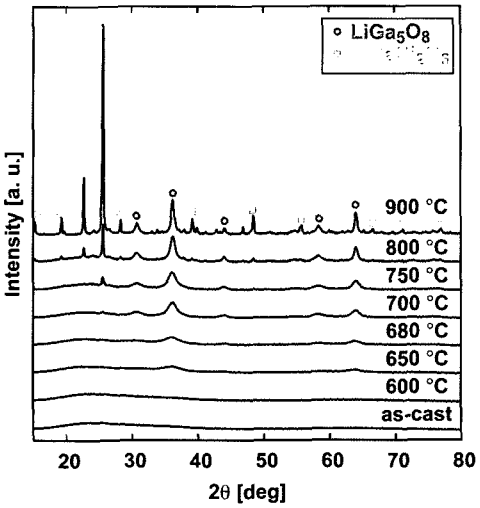

Fig. 2. The change of XRD patterns of Ni-doped Li_2O-Ga_2O_3-SiO_2 glass with the heat treatment temperature[7].

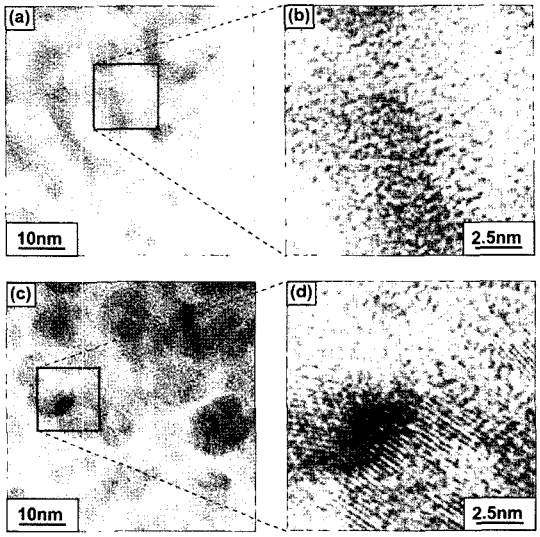

Fig. 3. Transmission electron microscope images as-quenched glass (a)(b) and glass-ceramic heat-treated at 680 °C (c)(d)[10].

ried out for 10 h. For the as-quenched sample and the sample heat-treated at 600 °C, a very weak and broad diffraction peak was observed around 2Θ=36°, which is the highest diffraction peak position of $LiGa_5O_8$(ICDD, #76-0199). This is consistent with the fact that as-quenched Li_2O-Ga_2O_3-SiO_2 glasses containing $LiGa_5O_8$ embryos[8,9]. In XRD patterns of the samples heat-treated at 650 and 680 °C, some weak and broad diffraction peaks attributable to inverse-spinel type $LiGa_5O_8$ were observed. These heat-treated glass-ceramics were transparent even after the heat treatment. In XRD patterns of the samples heat-treated at temperatures of 700 °C and higher, sharp and narrow peaks attributable to spodumene type $LiGaSi_2O_6$ (#26-0845) were seen in addition to peaks due to $LiGa_5O_8$. These heat-treated samples were not transparent.

Fig. 3 shows transmission electrom microscope images of as-cast glass and glass heat-treated at 680 °C. For as-cast glass, the contrast of magnitude of 10 nm shows phase separation of the glassy phases. Contrast of magnitude of 10 nm for heat-treated glass would be caused by crystalline phase because lattice fringes were clearly seen in Fig. 3 (d). The diameter of $LiGa_5O_8$ was roughly estimated to be about 10 nm from XRD and TEM.

Since the average diameter of $LiGa_5O_8$ is far smaller than the order of the wavelength of the visible and near-infrared photons, the scattering loss due to the difference of the refractive indices between crystallites and glass-matrix would become negligibly small. The samples heat-treated at 923 and 953 K, therefore, kept the transparency after heat treatment. In contrast, the average diameter of $LiGaSi_2O_6$ estimated from the XRD peak was about 100 nm for the sample heat-treated at 1173 K. This value is comparable to the wavelength of the visible and near-infrared photons, and therefore, serious scattering is caused by crystallites. These results show that heat treatment in the temperature range of 923 – 953 K is suitable to obtain transparent glass-ceramics because $LiGa_5O_8$ was the sole crystalline phase precipitated in the glass and the crystallite size was enough small to keep transparency for the visible and the near-infrared photons under such heat treatment conditions.

4. Optical Characterizations of Nickel-doped Transparent Glass-ceramics

4.1 UV-VIS-NIR Absorption

Glass and glass-ceramic were transparent but the color was changed drastically from amber to light blue by heat treatment. Fig. 4 shows UV-VIS-NIR spectra of as-cast glass and glass-ceramic heat-treated at 680 °C. As-quenched glass sample has three absorption bands located about 430, 860 and 1680 nm. The absorption spectrum of as-quenched sample is similar to that of

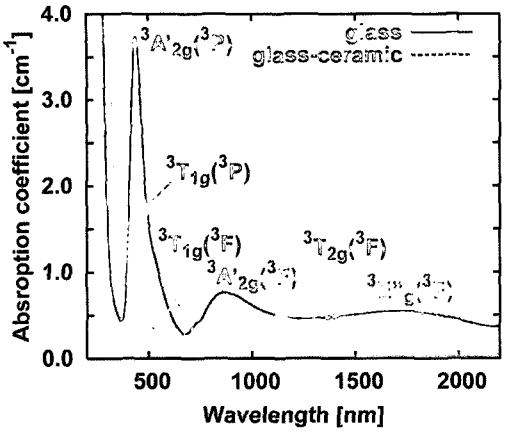

Fig. 4. Absorption spectra of as-cast glass and glass-ceramic heat-treated at 680 °C[5].

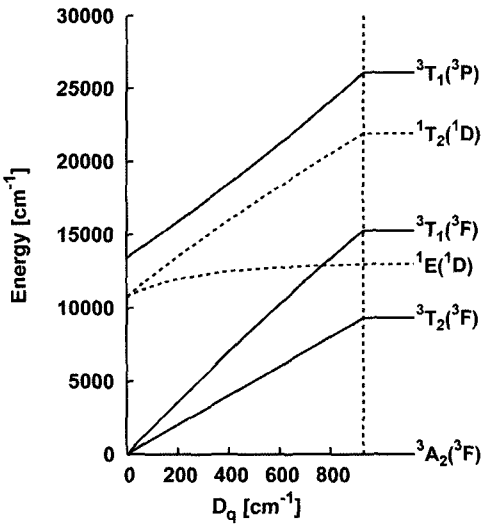

Fig. 5. Energy level diagram of octahedral Ni^{2+} in Li_2O-Ga_2O_3-SiO_2 glass-ceramic.

trigonal bipyramidal five-folded Ni^{2+}[11]. The 430, 860 and 1680 nm bands can be attributed to the transitions of $^3E_g'(^3F) \rightarrow {}^3A_{2g}'(^3P)$, $^3E_g'(^3F) \rightarrow {}^3A_{2g}'(^3F)$ and $^3E_g'(^3F) \rightarrow {}^3E_g''(^3F)$, respectively. The absorption spectra of bulk samples heat-treated for more than three hours are very similar to that of Ni: $LiGa_5O_8$. This shows that Ni^{2+} is incorporated into $LiGa_5O_8$crystallites during heat treatment. The absorption bands located around 380, 630 and 1060 nm can be attributed to the spin allowed transition of $^3A_{2g}(^3F) \rightarrow {}^3T_{1g}(^3P)$, $^3A_{2g}(^3F) \rightarrow {}^3T_{1g}(^3F)$ and $^3A_{2g}(^3F) \rightarrow {}^3T_{2g}(^3F)$ of octahedral six-folded Ni^{2+}, respectively. Two shoulder bands located around 450 and 770 nm can be attributed to the spin forbidden transition of $^3A_{2g}(^3F) \rightarrow {}^1T_{2g}(^1D)$ and $^3A_{2g}(^3F) \rightarrow {}^3E_g(^1D)$, respectively. The large difference of absorption spectra of as-quenched and heat-treated samples shows that Ni^{2+} in as-quenched samples is not necessarily incorporated into $LiGa_5O_8$ embryos.

The Racah parameter *B* and *C*, and crystal field strength parameter *Dq* of octahedral Ni^{2+} in the glass-ceramic estimated by fitting the absorption peaks to Tanabe-Sugano diagram[12] were *B*=895 cm^{-1}, *C*=3151 cm^{-1} and *Dq*=948 cm^{-1}. These values considerably agreed well with *B*=900 cm^{-1}, *C*=3150 cm^{-1} and *Dq*=977 cm^{-1} of Ni:$LiGa_5O_8$ at 70 K[13]. This suggests that the nanocrystals precipitated by annealing are $LiGa_5O_8$ incorporating Ni^{2+}. Fig. 5 shows energy level diagram of octahedral Ni^{2+} in the glass-ceramic.

4.2 Near-infrared Emission

No near-infrared emission was observed from as-quenched glass irrespective of excitation wavelengths. In contrast, strong near-infrared emission was observed from heat-treated glass-ceramic by the 976 nm excitation as shown in Fig. 6. The width of the near-infrared emission was about 300 nm that is about 8 times broader than the typical bandwidth of the 1.5 μm emission of erbium doped in glasses. The wavelength region from the O-band to L-band (1260-1625 nm) in optic communication systems is covered with the emission bandwidth. This suggests that the Ni^{2+}-doped glass-ceramic appears promising for use as ultra-broadband gain media.

Fig. 7 shows decay curves of near-infrared emission of Li_2O-Ga_2O_3-SiO_2 glass-ceramic. The emission decay curves of glass-ceramic had strong non-exponential characteristics though that of $LiGa_5O_8$ can be fitted well to an exponential function. This non-exponential characteristics of the decay curves are caused probably due to the site-to-site variations of Ni^{2+} ion in glass-ceramic.

Fig. 8 shows temperature dependence of near-infrared emission lifetime of Li_2O-Ga_2O_3-SiO_2 glass-ceramic. The lifetime of glass-ceramic given here is the mean duration defined by $\int_0^\infty tI(t)dt \Big/ \int_0^\infty I(t)dt$, where *t* and *I*(*t*) is time and the emission intensity, respectively. The lifetime was about 970 μsec at 5 K. Though it decreased gradually with increasing temperature and it was as high as 580 μsec even at 300 K, but it still about three times

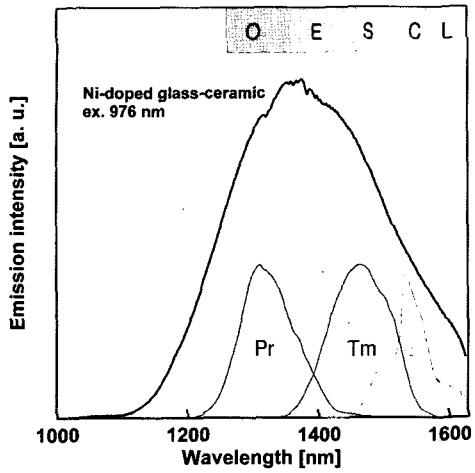

Fig. 6. Near-infrared emission spectrum of Ni-doped Li_2O-Ga_2O_3-SiO_2 glass-ceramic.

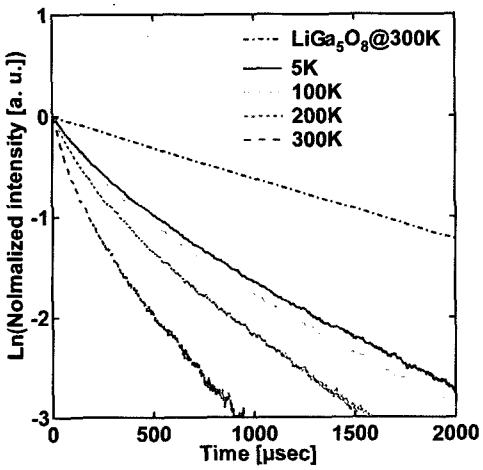

Fig. 7. Decay curves of near-infrared emission of Ni-doped Li_2O-Ga_2O_3-SiO_2 glass-ceramic.

shorter than that of $LiGa_5O_8$. This indicates that the origin of the non-radiative de-excitation of the glass-ceramic was not similar to that of Ni^{2+}:$LiGa_5O_8$ single crystal. The non-radiative de-excitation processes in the glass-ceramic may be enhanced by imperfections of crystallites grown from solid phase at low temperatures or some disturbing effects caused by adjacent glassy phase.

The quantum efficiency of near-infrared emission of glass-ceramic measured by an integration sphere method was 10 ± 2 % which is higher than about 1 % of Ni-doped ZnO-Al_2O_3-SiO_2 glass-ceramic and about 3 % of the O-band emission of Pr^{3+}-doped fluoride glass[15]. The quantum efficiency of Ni^{2+}:$LiGa_5O_8$ is, however,

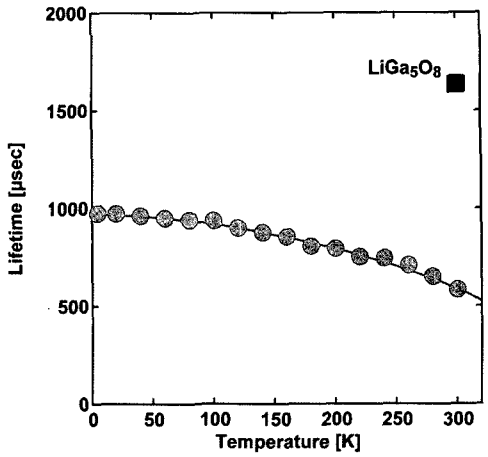

Fig. 8. Temperature dependence of lifetime of near-infrared emission of Ni-doped Li_2O-Ga_2O_3-SiO_2 glass-ceramic.

almost 100 % at room temperature. There is still room for improvement of the quantum efficiency of Li_2O-Ga_2O_3-SiO_2 glass-ceramic by optimization of preparation conditions such as glass compositions, heat treatment temperature and heat treatment duration etc.

The stimulated emission cross section can be estimated from the following equation assuming a Gaussian shape spectrum:

$$\sigma = \frac{\lambda_0^2 \eta}{4\pi n^2 \tau} \times \left(\frac{\ln 2}{\pi}\right)^{1/2} \times \frac{1}{\Delta \nu_{1/2}} \qquad (4\text{-}1),$$

where λ_0 is the band center wavelength, η is the quantum efficiency, n is the refractive index of host material, τ is the emission lifetime and $\Delta\nu_{1/2}$ is FWHM of the emission. Using this equation, the estimated stimulated emission cross section of the glass-ceramic was estimated to be 7.2×10^{-22} cm^2 at the peak.

The product of the stimulated emission cross section (σ) and the lifetime (τ) can be used as a figure of merit of optical gain and laser media because gain of an optical fiber amplifier is proportional to the $\sigma\tau$ and the threshold of laser oscillation is inversely proportional to the $\sigma\tau$. The $\sigma\tau$ of the glass-ceramic was about 4×10^{-25} $cm^2 \cdot sec$ which is as high as 6×10^{-25} $cm^2 \cdot sec$ for the S-band emission of Tm-doped glasse[16] and 4×10^{-25} $cm^2 \cdot sec$ for the O-band emission of Pr-doped glasses. This high figure of merit shows Ni-doped Li_2O-Ga_2O_3-SiO_2 glass-ceramic is a promising material for tunable lasers and broadband optical amplifiers for the wavelength division multiplexing transmission systems.

4.3 Excited State Absorption

Excited state absorption (ESA) cancels out optical gain when the ESA band overlaps with the emission band. In particular, ESA is a critical problem for transition metal ions doped materials, because electron-phonon coupling can broaden not only emission bands but also ESA bands of the transition metal ions. For octahedrally coordinated Ni^{2+}, the upward $^3T_{2g}(^3F) \rightarrow {}^3T_{1g}(^3F)$ transition of Ni^{2+} may overlap with the downward $^3T_{2g}(^3F) \rightarrow {}^3A_{2g}(^3F)$ transition. For example, it was reported that the $^3T_{2g}(^3F) \rightarrow {}^3T_{1g}(^3F)$ ESA band prevents lasing of the $^3T_{2g}(^3F) \rightarrow {}^3A_{2g}(^3F)$ transition in $Ni:MgAl_2O_4$ at room temperature[18]. In the case of Ni-doped Li_2O-Ga_2O_3-SiO_2 glass-ceramic case, the energy gap between $^3T_{2g}(^3F)$ and $^3T_{1g}(^3F)$ corresponds to the photon wavelength of 1547 nm and the net gain around this wavelength may decrease due to the ESA.

5. Summary

The structural and optical properties Ni-doped transparent glass-ceramics were reviewed. The quantum efficiencies of Ni-doped oxide crystals were examined to explore suitable crystalline phase for Ni-doping in glass-ceramic. The results showed that Ni doped in $LiGa_5O_8$ has very high quantum efficiency at room temperature.

Transparent glass ceramics containing $LiGa_5O_8$ was successfully synthesized by heat treatment of Li_2O-Ga_2O_3-SiO_2-NiO glass. The average size of precipitated crystals in the glass-ceramic was about 10 nm. Similarity of optical absorption spectra of the glasspceramic and Ni^{2+}:$LiGa_5O_8$ corresponds to that Ni^{2+} in glass-ceramic was incorporated into $LiGa_5O_8$ nanocrystals. The near-infrared emission covering from the O-band to L-band was observed from the glass-ceramic by the 976 nm excitation. The emission quantum efficiency was evaluated as about 10 % by an integration sphere method. The figure of merit as gain media was about 4×10^{-25} cm^2 · sec which is as high as thouse of rare-earth-doped glasses. The broad bandwidth and high quantum efficiency show that transparent glass-ceramics containing Ni^{2+}:$LiGa_5O_8$ nanocrystals are promising candidate novel ultra-broadband gain media.

Acknowledgments

The authors would like to thank Dr. G. Senthil Murugan and Yoshihide Nakatsubata for their contributions. This work was supported in part by MEXT, the Private University High-Tech Research Center Program (2002-2006, 2006-2010).

References

1. Y. Suzuki, W. Al. Silbey, O. H. El Bayoumi, T. M. Roberts, B. Bendow, Phys. Rev. B 35 (1987) 34.
2. B.N. Samson, L.R. Pinckney, J. Wang, H. Beall, N.F. Borrelli, Opt. Lett. 27 (2002) 1309.
3. T. Suzuki, Y. Ohishi, Appl. Phys. Lett. 84 (2004) 3804.
4. T. Suzuki, Y. Ohishi, in: Tech. Digest of Conf. on Lasers and Electro Optics, 2004, p. CTuD6.
5. T. Suzuki, G.S. Murugan, Y. Ohishi, Appl. Phys. Lett. 86 (2005) 131903.
6. T. Suzuki, G.S. Murugan, Y. Ohishi, in: Tech. Digest of Conf. on Lasers and Electro Optics, 2005, p. CME7.
7. T. Suzuki, Y. Arai, Y. Ohishi, J. Non-Cryst. Solids, 353 (2007) 36.
8. K. Tanaka, T. Mukai, T. Ishihara, K. Hirao, N. Soga, S. Sogo, M. Ashida, R. Kato, J. Am. Ceram. Soc. 76 (1993) 2839.
9. I. Yamaguchi, K. Tanaka, K. Hirao, N. Soga, J. Mater. Sci. 31 (1996) 3541.
10. T. Suzuki, Y. Arai, Y. Ohishi, submitted.
11. L. Galoisy, G. Calas, Geochim. Cosmochim. Acta 57 (1993) 3613.
12. Y. Tanabe, S. Sugano, J. Phys. Soc. Jpn. 753 (9) (1954) 766.
13. J.F. Donegan, F.J. Bergin, T.J. Glynn, G.F. Imbush, J.P. Remeika, J. Lumin. 35 (1986) 57.
14. M. Inokuti and F. Hirayama, J. Chem. Phys., 43 (1965) 1978.
15. Y. Ohishi, M. Yamada, A. Mori, T. Kanamori, M. Shimizu, S. Sudo, Opt. Lett., 20 (1995) 383.
16. J. Song, J. Heo, S. H. Park, J. Appl. Phys., 93 (2003) 9441.
17. Y. Ohishi, T. Kanamori, T. Kitagawa, S. Takahashi, E. Snitzer, G. H. Sigel, Jr., Opt. Lett., 16, 1747 (1991), Y. Ohishi, M. Yamada, A. Mori, T. Kanamori, M. Shimizu, S. Sudo, Opt. Lett., 20, 383 (1995).
18. N. V. Kuleshov, V. G. Shcherbitsky, V. P. Mikhailov, S. Kuck, J. Koetke, K. Petermann, G. Huber, J. Lumin., 71 (1997) 265.